

## Domain walls at the spin-density-wave endpoint of the organic superconductor (TMTSF)<sub>2</sub>PF<sub>6</sub> under pressure

N. Kang,<sup>1</sup> B. Salameh,<sup>1,2</sup> P. Auban-Senzier,<sup>1</sup> D. Jérôme,<sup>1</sup> C. R. Pasquier,<sup>1</sup> and S. Brazovskii<sup>3</sup>

<sup>1</sup>Laboratoire de Physique des Solides, UMR 8502-CNRS, Université Paris-Sud, Orsay F-91405, France

<sup>2</sup>Department of Applied Physics, Tafila Technical University, Tafila, Jordan

<sup>3</sup>LPTMS-CNRS, UMR 8626, Université Paris-Sud Bat 100, Orsay F-91405, France

(Received 16 December 2009; published 19 March 2010)

We report a comprehensive investigation of the organic superconductor (TMTSF)<sub>2</sub>PF<sub>6</sub> in the vicinity of the endpoint of the spin-density-wave metal phase transition where phase coexistence occurs. At low temperature, the transition of metallic domains toward superconductivity is used to reveal the various textures. In particular, we demonstrate experimentally the existence of one-dimensional and two-dimensional (2D) metallic domains with a crossover from a filamentary superconductivity mostly along the  $c^*$  axis to a 2D superconductivity in the  $b'c$ -plane perpendicular to the most conducting direction. The formation of these domain walls may be related to the proposal of a soliton phase in the vicinity of the critical pressure of the (TMTSF)<sub>2</sub>PF<sub>6</sub> phase diagram.

DOI: [10.1103/PhysRevB.81.100509](https://doi.org/10.1103/PhysRevB.81.100509)

PACS number(s): 74.70.Kn, 73.23.-b, 73.50.-h, 73.61.-r

Understanding the evolution from a magnetically ordered metallic (possibly insulating) ground state to a paramagnetic and metallic ( $M$ ) (potentially superconducting) ground state is a long-standing problem in condensed-matter physics. Such a situation is encountered in very diverse systems such as heavy fermion compounds, cuprates, and the recently discovered pnictide superconductors. In all these systems the parameter controlling the phase stability can be a dopant concentration, pressure, or magnetic field. Pressure was also at the origin of the discovery of superconductivity (SC) in the quasi-one-dimensional charge-transfer salt, (TMTSF)<sub>2</sub>PF<sub>6</sub>, where an insulating itinerant antiferromagnetic phase known as a spin-density-wave (SDW) ground state is stabilized at low temperature through a second-order phase transition. As the magnetic order can be driven to zero temperature by pressure with the stabilization of SC above  $P_c \approx 9$  kbar, one would be entitled to believe that the (TMTSF)<sub>2</sub>PF<sub>6</sub> phase diagram provides a good experimental playground for the study of a SDW quantum critical point. The study of the border region between SDW and SC becomes therefore an important issue for organic superconductivity since no consensus exists yet regarding the pairing mechanism and there has been a proposal for a microscopic coexistence of magnetic and superconducting order in a narrow pressure domain implying non-nested region on the Fermi surface in the vicinity of the boundary  $P_c$ .<sup>1</sup> Early studies<sup>2,3</sup> recognized that the transition from the SDW to the metallic state is of first order in this pressure regime which has been in turn extensively revisited by various techniques in the last decade. Resistivity measurements were performed by Vuletic *et al.*<sup>4</sup> making small pressure increments up to  $P_c$  and subsequently by Kornilov *et al.*<sup>5</sup> at a fixed pressure but monitoring the distance to  $P_c$  via an applied magnetic field. Both studies concluded to the coexistence of the two phases SDW/ $M$  or SDW/SC although in spatially separated regions. The possibility of metallic slabs becoming superconducting at low temperature in the pressure regime where  $T_c$  remains constant was suggested by transport data along the most conducting axis and also supported by a drastic enhancement of the upper critical field.<sup>6-8</sup> Furthermore, Vuletic *et al.*<sup>4</sup>

pointed out the existence of a particular pressure,  $P_{c0}$ , related to a sudden vanishing of SC coherence. Simultaneous measurements of NMR and transport at a given pressure have corroborated the claims for macroscopic coexistence coming from transport data and have also provided an analysis of the volume fraction as a function of temperature.<sup>9,10</sup> However, the comprehensive pressure mapping of this coexistence regime SDW- $M$ (SC) in the  $P$ - $T$  phase diagram is still missing as well as how the minority phase  $M$  self-organizes within the majority SDW phase. On theoretical grounds, various approaches have been developed: Ginzburg-Landau-like models have succeeded to obtain a phase coexistence between SC and SDW states<sup>11</sup> and a modulation of the SC and SDW order parameters along both  $a$  and  $b$  axes has been suggested.<sup>12</sup> A microscopic approach has also been developed<sup>13,14</sup> based on the soliton theory which leads to a modulation of the SC and SDW order parameters along the  $a$  axis.

In this Rapid Communication, we explore the emergence of the minority phase, metallic (or SC at low temperature) from the pure SDW state and how it evolves toward the homogeneous metal (or SC) state under pressure. We use superconductivity as a tool to decorate the texture by comparing the temperature dependence of resistivity experiments performed along the  $a$ ,  $b'$ , and  $c^*$  axes. This texture is in favor of the soliton model.

Resistivity measurements were performed in high-quality (TMTSF)<sub>2</sub>PF<sub>6</sub> single crystals from the batch used in an earlier study.<sup>4</sup> Gold-plated electrical contacts were evaporated on the sample surfaces to measure  $\rho_a$ ,  $\rho_b$ , and  $\rho_c$  along  $a$ ,  $b'$ , and  $c^*$  axes, respectively, on different samples. The resistance measurements were performed using a standard low-frequency lock-in detection. The applied current was chosen in order to remain below the SC critical current along the considered axis for each pressure and to minimize heating effects. The measurements were carried out in a dilution refrigerator ( $T \geq 50$  mK) with a magnetic field always applied along the  $c^*$  axis. Measuring the resistivity tensor on the same sample would have obviously been the most satisfactory solution but this happens to be nonfeasible. Indeed, con-

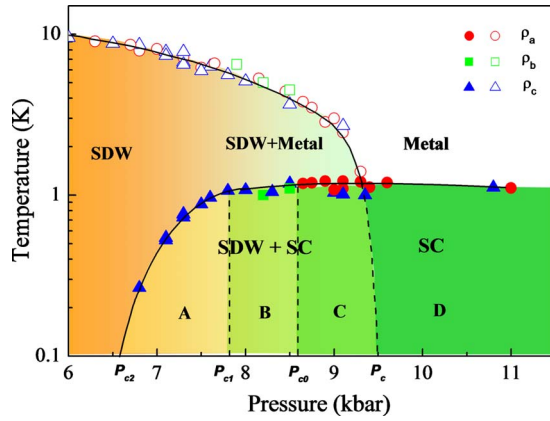


FIG. 1. (Color online) Phase diagram of  $(\text{TMTSF})_2\text{PF}_6$  as determined from resistivity measurements along the three axes (circles:  $\rho_a$ ; squares:  $\rho_b$ ; triangles:  $\rho_c$ ). The filled (open) symbols correspond to the transition toward SC (SDW), respectively. The contrast of colors between  $P_{c2}$  and  $P_c$  illustrates the increase in SC volume fraction from  $P_{c2}$  up to  $P_c$  corresponding to the three different regimes explained in the text. Based on the knowledge of  $T_{SDW}$  and  $T_c$ , the pressure of 5.5 kbar in Ref. 9 would correspond to 8.8 kbar with the present pressure scale.

tacts evaporated on the crystal surfaces for the measurement along a given axis always short circuit and consequently preclude measurements along a perpendicular axis. For a comparison of the transport anisotropy at a given pressure  $P$ , we chose among our various pressure runs the ones corresponding to  $P \pm 0.1$  kbar. Hydrostatic pressures up to 11 kbar were generated by using a Be-Cu clamp cell with Daphné silicon oil as the pressure transmitting medium. Given the importance to study transport along the three axes at the same pressure, a determination of the pressure or at least of the relative pressure between different runs is of crucial importance for the present study. This was achieved at low temperature using as an *in situ* pressure gauge, the pressure dependence of the sharp SDW transition reported in Vuletic *et al.*<sup>4</sup> The main result of this Rapid Communication is the establishment of a detailed phase diagram for the coexistence region which is displayed on Fig. 1. As shown in this Fig. 1, the domain of the  $(\text{TMTSF})_2\text{PF}_6$  phase diagram where SC is observed can be subdivided into four different regions according to the response of transport to SC along the different axes. In particular, the SDW/M(SC) phase coexistence is observed between  $P_{c2}=6.6$  kbar and  $P_c=9.4$  kbar with a strong increase in the critical temperature between  $P_{c2}$  and  $P_{c1}=7.8$  kbar (phase A), a much weaker one between  $P_{c1}$  and  $P_{c0}$  (phase B) and finally  $T_c$  remains pressure independent above  $P_{c0}$  (phase C).

Phase A,  $P_{c2}=6.6 < P < P_{c1}=7.8$  kbar as shown in Fig. 2(a), while the resistivities along the three axes exhibit similar insulating temperature dependences for  $T > 1\text{K}$ , only  $\rho_c$  exhibits a partial SC transition. In contrast,  $\rho_a(T)$  exhibits the same insulating behavior as in the low pressure purely SDW state over the whole measured  $T$  range.  $\rho_b(T)$  follows  $\rho_a(T)$  except near  $P_{c1}$  where it exhibits a saturation at low temperatures. The  $T_c^{\text{onset}}(P)$ , in Fig. 1, is defined by the onset of superconductivity, namely, the maximum of  $\rho_c(T)$  at a given

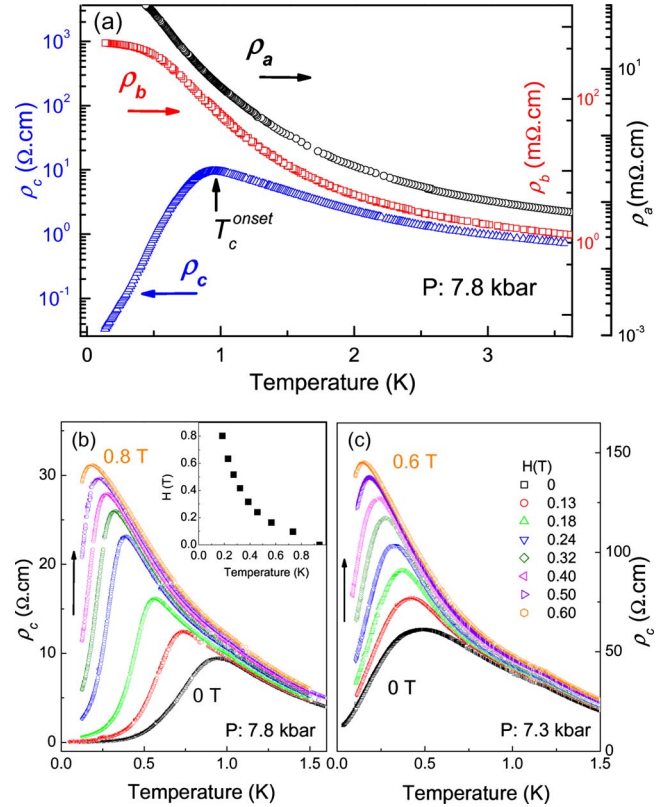


FIG. 2. (Color online) Phase A: (a) temperature dependence of  $\rho_a$ ,  $\rho_b$ , and  $\rho_c$  at  $P=7.8$  kbar. (b) Temperature dependence of  $\rho_c$  at  $P=7.8$  kbar for magnetic fields ranging from 0 to 0.8 T by step of 0.1 T. The insert shows the deduced upper critical field line. (c) Temperature dependence of  $\rho_c$  at  $P=7.3$  kbar for different magnetic fields.

pressure, see Fig. 2(a). The sensitivity of SC to magnetic field is shown in Figs. 2(b) and 2(c) by the evolution of  $\rho_c(T)$  with the applied magnetic field at  $P=7.3$  kbar and  $P=7.8$  kbar. The upward curvature of the upper critical field down to the lowest temperatures is in agreement with previous reports in  $(\text{TM})_2\text{X}$  salts.<sup>6–8</sup> In this phase A, a higher pressure increases  $T_c$  and reduces the broadness of the transition. Such a behavior is typical of phase separation as long as SC domains are smaller than the penetration depth. Our data are also compatible with the formation of filaments elongated mainly along the  $c^*$  axis which may cross the whole thickness of the sample approaching  $P_{c1}$ . Indeed, our observations looks qualitatively similar to the results for SC wires<sup>15</sup> where the inherent presence of phase slips gives rise to finite resistance below  $T_c$ .

Phase B,  $P_{c1}=7.8 < P < P_{c0}=8.6$  kbar: as shown in Figs. 3 and 4, both  $\rho_b(T)$  and  $\rho_c(T)$  exhibit a SC transition. The drop of  $\rho_b$  to a finite resistance state reproduces the broad decrease in  $\rho_c(T)$  at  $T_c^{\text{onset}}(P)$  and can be attributed to the SC transition in the metallic domains, coexisting with the SDW background. At lower temperatures, the increase in  $\rho_b(T)$  infers that SDW domains are in series with SC domains along  $b'$ . A (true) zero resistance state along  $c^*$  axis is achieved, in phase B, at a temperature which increases with pressure. However, at both  $P=8.0$  kbar and  $P=8.3$  kbar,  $\rho_a$  still remains insulating. Therefore, the system looks like an array of

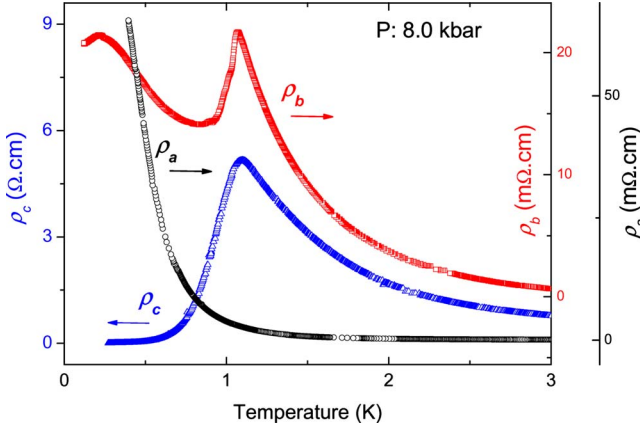


FIG. 3. (Color online) Phase B,  $P=8.0$  kbar: temperature dependence of  $\rho_a$ ,  $\rho_b$ , and  $\rho_c$  at zero magnetic field.

SC-SDW-SC junctions with Josephson coupling across insulating barriers, all located in  $b'c$  planes. The in-plane Josephson coupling increases with higher pressure or lower temperature leading to superconducting correlation in the  $b'$  direction and in turn to 2D SC within  $b'c$  planes. Hence, below  $\sim 0.2K$ , an enhanced Josephson coupling allows a weak decrease in  $\rho_b(T)$  at  $P=8.0$  kbar which shifts to larger temperatures upon increasing pressure, that is,  $\sim 0.76K$  at

$P=8.3$  kbar. The existence of SC along the  $b'$  axis is confirmed by the disappearance of SC under a finite magnetic field as shown in Fig. 4(b). This phenomenon is typical of granular superconductors and superconductor-insulator transition systems<sup>16</sup> and disappears at  $P_{c0}$  where both  $\rho_b(T)$  and  $\rho_c(T)$  present a (single) sharp transition at  $T_c^{onset}(P)$ . The 2D nature of SC in phase B is confirmed on Fig. 4(a) by the fit of the  $\rho_b(T)$  curve below  $T_{2D} \sim 0.45K$  by a model considering a 2D SC above its Berezinskii-Kosterlitz-Thouless (BKT) transition temperature,  $T_{BKT} \sim 0.15K$ , where the resistance reads,  $R_{BKT}(T) = R_0 \exp[-(G_i^{2D} \frac{T_{BKT}}{T - T_{BKT}})^{1/2}]$ , where  $G_i^{2D} \sim T_{BKT} / \sqrt{t_b t_c}$  is the 2D Ginzburg parameter and  $R_0$ , a fitting parameter.<sup>17</sup>

Phase C,  $P_{c0} = 8.6 < P < P_c = 9.4$  kbar: both  $\rho_b(T)$  and  $\rho_c(T)$  present a sharp transition at  $T_c^{onset}(P)$  with a zero resistance state below  $T_c^{onset}(P)$ .  $\rho_a(T)$  data have been already presented:<sup>4</sup> the pressure evolution of  $\rho_a$  mimics the evolution of  $\rho_b$  in phase B. In particular, a “double transition” in  $\rho_a(T)$  is observed nearly up to  $P_c$ .

Phase D. superconductivity appears to be homogeneous above  $P_c = 9.4$  kbar.

The starting frame of any interpretation is the electronic zone in the reciprocal lattice with the electronic spectrum  $E(\vec{k})$  satisfying the nesting condition  $E(\vec{k} + \vec{Q}) \approx -E(\vec{k})$  (with the accuracy of  $\Delta$  since at low  $T$  the state is insulating). The commonly used model limits the major spectrum also to only nearest neighbors overlaps:  $E(\vec{k}) = -2t_a \cos k_a - 2t_{b0} \cos k_b$  leading to the common-sense nesting wave number  $\vec{Q}_0 = 2\pi(1/2, 1/2, 1/2)$ . (The wave numbers,  $k_i$ , are taken in units of inverse lattice parameters.) But the SDW was always recognized to be incommensurate, and moreover its wave number has been well determined, in  $a$  and  $b$  directions, as  $\vec{Q}_{SDW} = 2\pi(1/2, q_b, q_c)$ —with  $q_b = 1/4 \pm 0.05$ , not  $1/2$ . These direct x-ray results<sup>18</sup> agree with simulations from the NMR studies<sup>19,20</sup> giving  $q_b$  as 0.2 or 0.3. That was elucidated by band structure calculations<sup>21</sup> as an ill-expected interference of oblique interstack overlaps,  $t_{b1}$  between the nearest molecular stacks in  $b$  direction but among molecules which are next-nearest neighbors along the stack:  $E(\vec{k}) = -2t_a \cos k_a - 2t_{b0} \cos k_b - 2t_{b1} \cos(k_b - k_a)$ . Having written it,<sup>1</sup> at the Fermi sheets  $k_a \approx \pm \pi/2$ , as  $E(\vec{k}) = \pm v_F \delta k_a - 2t_b(k_a) \cos(k_b \mp \Phi_0)$ ,  $\Phi_0 = \pm \arctan(t_{b1}/t_{b0})$ , one sees that the interference does not destroy the nesting but shifts its vector, in  $b$  direction, from  $\pi$  to  $q_b = \pi - 2\Phi_0$ . For room-temperature crystal parameters the effect is small as expected, but, at low  $T$ , it becomes as large<sup>21</sup> as to shift  $q_b$  from  $1/2$  to the vicinity of  $1/4$ .

The metallization and progressive destruction of the SDW state is determined by the antinesting energy  $E_{anti}(\vec{k}) = [E'(\vec{k}) + E'(\vec{k} + \vec{Q})]/2$ . It is given by the smaller contributions  $E'(\vec{k}) = -2t_c \cos k_c - 2t'_b \cos 2k_b$  considering them at the new nesting vector  $\vec{Q}$  as it is determined by the dominant term. The conventional candidate for un-nesting,  $-2t'_b \cos 2k_b$ , gives  $E_{anti}^b(\vec{k}) = -t'_b [\cos 2k_b + \cos(2k_b + 4\pi q_b)]$ . For the commonly supposed  $q_b = 1/2$ , the two terms are identical giving  $E_{anti}^b(\vec{k}) = -2t'_b \cos 2k_b$ . But now, for  $q_b = 1/4$ , the two terms have opposite signs, so  $E_{anti}^b(\vec{k})$  just vanishes. Although  $q_b$  may not be exactly  $1/4$ , the incommensurability of

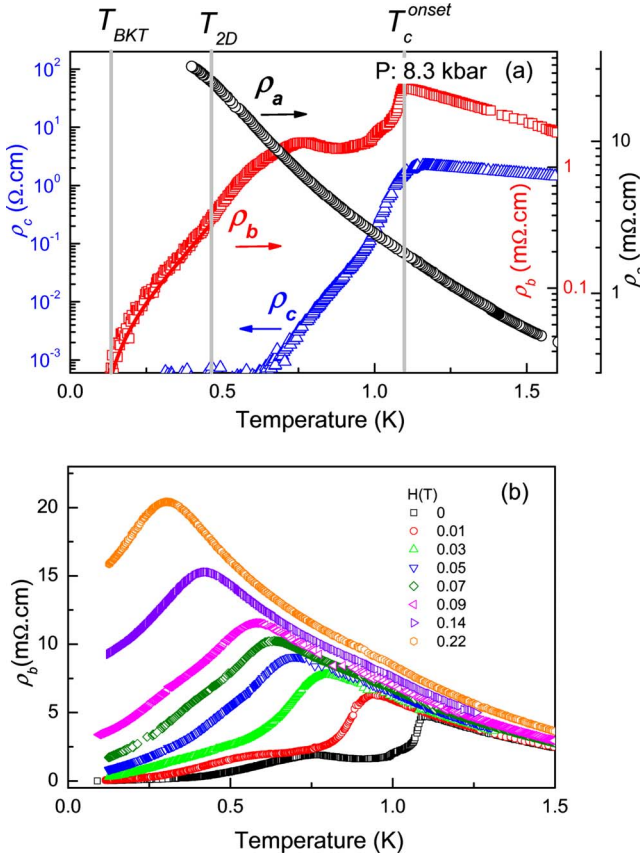


FIG. 4. (Color online) Phase B,  $P=8.3$  kbar: (a) temperature dependence of  $\rho_a$ ,  $\rho_b$ , and  $\rho_c$ . The line through the data points of  $\rho_b$  corresponds to the fit of  $\rho_b$  by the BKT model. (b) Temperature dependence of  $\rho_b$  for different magnetic fields.

the SDW induces a noticeable decrease in  $E_{anti}^b(\vec{k})$ . Also, the effect of oblique overlaps slightly decreases with pressure,<sup>21</sup> hence the compensation of un-nesting in  $b$  direction reduces and this direction starts to play a bigger role. That seems to correlate with our observations. The  $c$ -axis term,  $E_{anti}^c(\vec{k}) = -t_c[\cos k_c + \cos(k_c + 2\pi q_c)]$ , survives: even if  $q_c$  is not well determined, for all data  $q_c \neq 1/2$  (Refs. 18 and 20)—there are no major terms to fix it as it was for  $q_b$ . Therefore, most functions of the SDW destruction, formation of the solitonic midgap state or of spill-over pockets, and finally of stabilization of initially fragmented solitonic walls—all are maintained by electronic hybridization in the nominally weakest  $c$  direction. This picture is coherent with our observation, at first sight counterintuitive, that the SC develops first in the direction of worst conduction.

In conclusion, we have reported a comprehensive investigation of the coexistence region in the pressure-temperature phase diagram of (TMTSF)<sub>2</sub>PF<sub>6</sub> near the critical pressure  $P_c$ , in which the SC phase is inhomogeneous and spatially modulated. This regime is characterized by conducting (SC) slabs perpendicular to the most conducting axis which originate from the coalescence of metallic domains elongated

mainly along the  $c^*$  axis at low pressure as evidenced from the onset of superconductivity first along  $c^*$ , while the system remains insulating along the perpendicular directions. At increasing pressure, metallic (SC) coherence sets in along the  $b'$  direction as well. An improvement of the model, coherent to both new and old overlooked observations, is proposed to understand the counterintuitive experimental picture. Our study might be extended in the SDW/ $M$  regime above  $T_c$  as already suggested<sup>22</sup> even if the texture is more difficult to extract in this regime. The existence of a textured SC phase at the border of the SDW/metal transition in (TMTSF)<sub>2</sub>PF<sub>6</sub> could help to shed light on the nature of coexistence of two ordered phases in other strongly correlated systems, other (TM)<sub>2</sub>X salts as well as the recently discovered iron-pnictide superconductors.<sup>23</sup>

This work was supported by the European Community under the project CoMePhS (Grant No. NMPT4-CT-2005-517039). N.K. and B.S. also acknowledge financial support from this grant. S.B. acknowledges supports of the ANR program (Project No. BLAN07-3-192276).

- 
- <sup>1</sup>K. Yamaji, J. Phys. Soc. Jpn. **51**, 2787 (1982).  
<sup>2</sup>R. L. Greene and E. M. Engler, Phys. Rev. Lett. **45**, 1587 (1980).  
<sup>3</sup>R. Brusetti, M. Ribault, D. Jérôme, and K. Bechgaard, J. Phys. **43**, 801 (1982).  
<sup>4</sup>T. Vuletić, P. Auban-Senzier, C. Pasquier, S. Tomić, D. Jérôme, M. Héritier, and K. Bechgaard, Eur. Phys. J. B **25**, 319 (2002).  
<sup>5</sup>A. V. Kornilov, V. M. Pudalov, Y. Kitaoka, K. Ishida, G.-q. Zheng, T. Mito, and J. S. Qualls, Phys. Rev. B **69**, 224404 (2004).  
<sup>6</sup>I. J. Lee, P. M. Chaikin, and M. J. Naughton, Phys. Rev. Lett. **88**, 207002 (2002).  
<sup>7</sup>C. V. Colin, B. Salameh, C. R. Pasquier, and K. Bechgaard, J. Phys.: Condens. Matter **20**, 434230 (2008).  
<sup>8</sup>A.-S. Rüetschi and D. Jaccard, Eur. Phys. J. B **67**, 43 (2009).  
<sup>9</sup>I. J. Lee, S. E. Brown, W. Yu, M. J. Naughton, and P. M. Chaikin, Phys. Rev. Lett. **94**, 197001 (2005).  
<sup>10</sup>W. Yu, S. E. Brown, F. Zamborsky, I. J. Lee, and P. M. Chaikin, Int. J. Mod. Phys. B **16**, 3090 (2002).  
<sup>11</sup>D. Podolsky, E. Altman, T. Rostunov, and E. Demler, Phys. Rev. Lett. **93**, 246402 (2004).  
<sup>12</sup>W. Zhang and C. A. R. Sá de Melo, Phys. Rev. Lett. **97**, 047001 (2006).  
<sup>13</sup>S. A. Brazovskii, L. P. Gor'kov, and R. Schrieffer, Phys. Scr. **25**, 423 (1982); S. A. Brazovskii, L. P. Gor'kov, and A. Lebed, Sov. Phys. JETP **56**, 683 (1982).  
<sup>14</sup>L. P. Gor'kov and P. D. Grigoriev, Europhys. Lett. **71**, 425 (2005).  
<sup>15</sup>A. Bezryadin, C. N. Lau, and M. Tinkham, Nature (London) **404**, 971 (2000).  
<sup>16</sup>K. A. Parendo, K. H. Sarwa B. Tan, and A. M. Goldman, Phys. Rev. B **76**, 100508(R) (2007).  
<sup>17</sup>M. Tinkham, *Introduction to Superconductivity*, 2nd ed. (Dover, New York, 2004).  
<sup>18</sup>J.-P. Pouget and S. Ravy, Synth. Met. **85**, 1523 (1997).  
<sup>19</sup>J. M. Delrieu, M. Roger, Z. Toffano, A. Moradpour, and K. Bechgaard, J. Phys. **47**, 839 (1986).  
<sup>20</sup>T. Takahashi, Y. Maniwa, H. Kawamura, and G. Saito, J. Phys. Soc. Jpn. **55**, 1364 (1986).  
<sup>21</sup>L. Ducasse, M. Abderrabba, and B. Gallois, J. Phys. C **18**, L947 (1985); L. Ducasse, M. Abderrabba, J. Hoarau, M. Pesquer, B. Gallois, and J. Gaultier, *ibid.* **19**, 3805 (1986).  
<sup>22</sup>A. G. Lebed, Sov. Phys. JETP **59**, 909 (1984).  
<sup>23</sup>J. H. Chu, J. G. Analytis, C. Kucharczyk, and I. R. Fisher, Phys. Rev. B **79**, 014506 (2009).